第 35 卷第 3 期
2019 年 3 月

无 机 化 学 学 报
CHINESE JOURNAL OF INORGANIC CHEMISTRY

Vol.35 No.3
515-523

具有同质多晶现象的一维和二维锌(Ⅱ)配合物的水热合成及对苦味酸的可循环荧光检测性能

李欣書[1,2] 王 倩*[,1,2] 丁 斌*[,1,2]

([1]天津市功能分子结构与性能重点实验室,无机–有机杂化功能材料化学教育部重点实验室,天津师范大学化学学院,天津 300387)

([2]南开大学先进能源材料化学教育部重点实验室,天津 300071)

摘要:用一个具有双官能基团的半刚性多齿配体 5-(4-((1*H*-1,2,4-三唑-1-基)甲基)苯基)-1*H*-四唑(HL)与锌(Ⅱ)在水热条件下制备了 2 个具有同质多晶结构的锌(Ⅱ)配位聚合物,即[Zn(μ_2-L)$_2$]$_n$ (**1**)和[Zn(μ_2-L)$_2$]$_n$ (**2**)。配合物 **1** 和 **2** 代表了温度诱导形成的同质多晶结构的一维(**1**)和二维(**2**)锌(Ⅱ)-L 配位框架。在 **1** 中,一维左手和右手螺旋链相互连接,最终形成了一维锌(Ⅱ)-L 链配合物。在 **2** 中,这些一维左手和右手螺旋链也通过中心锌(Ⅱ)离子相互连接,形成二维的配位框架。研究了 HL 和配合物 **1**、**2** 的光致发光性质,结果表明它们都具有强的荧光发射峰。此外,光致发光实验还表明,配合物 **2** 在水溶液中对苦味酸表现出高灵敏度的发光检测,具有高猝灭效率(K_{sv}=3.65×10^3 L·mol^{-1})和低检测限(3.004 μmol·L^{-1},*S*/*N*=3),这使其可用来检测苦味酸。

关键词:水热;同质多晶;锌;荧光传感;苦味酸

中图分类号:O614.24$^+$1 **文献标识码**:A **文章编号**:1001-4861(2019)03-0515-09

DOI:10.11862/CJIC.2019.057

Polymorphic One- and Two-dimensional Zinc(Ⅱ) Coordination Polymers: Hydrothermal Preparation and Recyclable Photoluminescent Sensing for Picric Acid

LI Xin-Shu[1,2] WANG Qian*[,1,2] DING Bin*[,1,2]

([1]*Tianjin Key Laboratory of Structure and Performance for Functional Molecules, MOE Key Laboratory of Inorganic-Organic Hybrid Functional Material Chemistry, College of Chemistry, Tianjin Normal University, Tianjin* 300387, *China*)

([2]*Key Laboratory of Advanced Energy Materials Chemistry, Ministry of Education, Nankai University, Tianjin* 300071, *China*)

Abstract: A semi-rigid bi-functional multi-dentate ligand 5-(4-((1*H*-1,2,4-triazol-1-yl)methyl)phenyl)-1*H*-tetrazole (HL) has been employed to prepare two polymorphic zinc(Ⅱ) coordination polymers, namely [Zn(μ_2-L)$_2$]$_n$ (**1**) and [Zn(μ_2-L)$_2$]$_n$ (**2**) under hydrothermal conditions. Complexes **1** and **2** present temperature induced polymorphic zinc (Ⅱ)-L 1D (**1**) and 2D (**2**) coordination frameworks. In **1**, 1D left- and right-handed helical chains are inter-linked to form a 1D chain zinc(Ⅱ)-L coordination polymer. In **2**, these 1D left- and right-handed helical chains are also interlinked via central zinc(Ⅱ) ions forming the two-dimensional (2D) coordination framework. The photoluminescent properties of free HL and **1**~**2** have been investigated, indicating strong emissions. Additionally, photoluminescent experiment also demonstrates that complex **2** exhibits highly sensitive luminescence sensing for picric acid in the aqueous solutions with high quenching efficiency (K_{SV}=3.65×10^3 L·mol^{-1}) and low detection limit (3.004 μmol·L^{-1}, *S*/*N*=3), which make it a promising candidate for sensing picric acid. CCDC: 1865772, **1**; 1486544, **2**.

Keywords: hydrothermal; polymorphic; zinc; photo-luminescence sensing; picric acid

收稿日期:2018-09-13。收修改稿日期:2018-12-15。

国家自然科学基金(No.21301128),天津市自然科学基金(No.14JCQNJC05900),天津市高等学校创新团队培养计划(No.TD13-5074),111 引智基地(111 project,No.B12015)和天津师范大学大学生创新训练项目(No.201612)资助。

*通信联系人。E-mail:hxxywq@tjnu.edu.cn,hxxydb@mail.tjnu.edu.cn

0 Introduction

During the last two decades, rational design and syntheses of novel coordination polymers have received great interest because these materials can be widely utilized in gas storage/separation, drug delivery, photoluminescent materials and magnetic materials[1]. In general, the successful preparation of coordination polymers can be correlated with judicious selective of multi-functional ligands, secondary basic building units (SBUs) and various different reaction conditions[2]. Generally, flexible links can give rise to materials that demonstrate crystal-to-crystal breathing and complex adsorption effects such as gating, and sensing, where metal-organic frameworks respond to the nature and/or pressure of the adsorbate[3]. Link-derived dynamic behavior carefully controls the flexibility of the ligand. Thus, links with limited degrees of freedom have most successfully been employed in the synthesis of flexible metal-organic frameworks[4]. The integration of materials displaying advanced framework flexibility with photoluminescent responsive SBUs underlies one approach to sense and respond to small molecule adsorbents[5].

With the development of modern society and industry, hazardous chemicals, like toxic organic small molecules, are increasingly released from industrial facilities and other anthropogenic activities, which cause adverse effects on human health and the environment[6]. As a class of toxic and hazardous chemicals, nitro explosives should not be neglected. Picric acid (PA), as one of the common nitro explosives, is extensively applied in dyes, fireworks, and the pharmaceutical and leather industries[7]. Due to its frequent use, a large quantity of PA is released to the environment, which may cause serious health problems, such as gene mutation, injury to respiratory organs, anemia, and male infertility. Besides, PA has stronger explosive power than other common nitro explosives. Previously, some studies on luminescence-based detection of PA have been reported, especially with luminescent sensors, indicating the current topic has received great interest[8]. Consequently, it is necessary to develop convenient, fast, and highly efficient methods to detect PA in various samples with regard to environmental monitoring, homeland security, forensic science, and military applications[9].

We also are interesting in the construction of novel metal organic frameworks, which can be utilized as functional materials with intriguing magnetic and photoluminescent properties[10]. 1,2,4-Triazole, especially its derivatives, have the potential to bridge in bi-dentate and tri-dentate bridging fashions, which are expected to construct novel functional coordination polymers with intriguing structural motifs and novel functional properties[11]. On the other hand, tetrazole-based ligands are also a splendid option of N-donor ligands, and the four nitrogen atoms provide enough coordination sites when coordinating to metal centers with certain coordination geometries[12]. However, it is noted that the asymmetric semi-rigid bridging N-donor ligands, namely, the ligand possessing different N-containing coordination groups (such as the bi-functional ligands simultaneously containing triazole and tetrazole groups) have rarely been investigated. 5-(4-((1*H*-1, 2, 4-triazol-1-yl)methyl)phenyl)-1*H*-tetrazole (HL) simultaneously contains one triazole group, one aromatic benzene group and one tetrazole group. As a matter of fact, HL has six potentially coordinated N atoms in a molecule, which may exhibit various bridging modes. Additionally there also exist flexible dihedral angles between triazole, phenyl and tetrazole aromatic rings within HL (Scheme 1). The conformational freedom of these semi-rigid flexible ligands should provide more possibilities for the construction

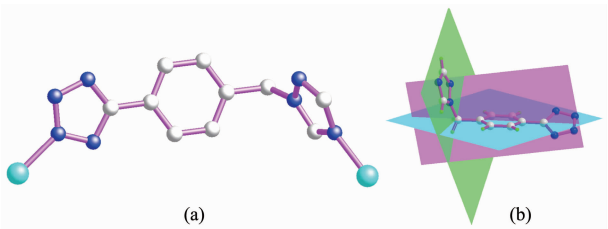

Color code: (a) Cyan: Metal, Blue: N; Light grey: C; (b) Green: triazole; Sky blue: phenyl, Pink: tetrazole

Scheme 1 (a) Bi-dentate coordination mode of flexible multi-dentate HL ligand; (b) Flexible dihedral angles between triazole, phenyl and tetrazole moieties within HL

of coordination polymers with interesting structures and appealing functional properties.

In this work, the semi-rigid HL containing bi-functional triazole and tetrazole moieties has been employed, and two polymorphic zinc(Ⅱ) coordination polymers, namely $[Zn(\mu_2\text{-}L)_2]_n$ (**1**) and $[Zn(\mu_2\text{-}L)_2]_n$ (**2**), have been isolated under the hydrothermal conditions. **1** and **2** present temperature induced polymorphic zinc(Ⅱ)-L 1D (**1**) and 2D (**1**) coordination polymers. Further photo-luminescence experiment illustrate that complex **1** exhibits highly sensitive luminescence for PA in aqueous solutions with high quenching efficiency (K_{SV}=3.65×10^3 L·mol^{-1}) and low detection limit (3.004 μmol·L^{-1}, *S*/*N*=3), which make it a promising candidate for sensing PA in the measurement process. The detection platform based on **1** has its own advantage in the detecting process of PA since it possess high K_{SV} value and low detection limit, additionally the detection method is simple, rapid, cost effectiveness and recyclable. The polymorphic phenomena about the sensing coordination polymer **1** also are scarcely reported.

1 Experimental

1.1 General

Ligand L was prepared according to the literature methods[13]. All the other reagents were commercially available and utilized without further purification. Perkin-Elmer 240 elemental analyzer was ulitilized to perform C, H and N microanalyses. FT-IR spectra (4 000~500 cm^{-1}) were recorded by utilizing a NICOLET 6700 FT-IR spectroscope with KBr pellets (NICOLET, USA). Powder X-ray diffraction analysis was performed on a D/Max-2500 X-ray diffractometer using Cu *K*α radiation (λ=0.154 1 nm, *U*=40 kV, *I*=40 mA) with a 2θ range of 5°~50°. Photoluminescent emission fluorescence spectra were recorded on a RF-5301 spectrophotometer (Shimadzu, Japan).

1.2 Preparation of complexes 1 and 2

A mixture of $Zn(NO_3)_2\cdot 6H_2O$ (29.8 mg, 0.1 mmol) and HL (44 mg, 0.2 mmol) in 10 mL H_2O was placed in a Teflon vessel in a steel autoclave, heated at 120 ℃ for 12 h and then cooled to room temperature over 72 h. The resulting colorless block-shaped crystals of **1** were washed several times by water and diethyl ether. Elemental analysis Calcd. for $C_{20}H_{16}N_{14}Zn$(%): C 46.39, H 3.11, N 37.87; Found (%): C 46.65, H 3.31, N 37.98. FT-IR (cm^{-1}, KBr): 3 387(m), 3 085(w), 2 924 (w), 1 604(m), 1 532(w), 1 369(w), 1 280(m), 1 134(s), 999(m), 863(m), 744(m), 700(w), 673(w), 633(w), 569(w).

Complex **2** was synthesized by the same methods as **1** except that different hydrothermal reaction temperature 160 ℃ was used. The resulting colorless block-shaped crystals of **2** were washed several times by water and diethyl ether. Elemental analysis Calcd. for $C_{20}H_{16}N_{14}Zn$(%): C 46.39, H 3.11, N 37.87; Found (%): C 46.68, H 3.38, N 37.96. FT-IR (cm^{-1}, KBr): 3 780 (m), 3 691(w), 3 445(s), 2 921 (m), 2 356(s), 1 594(m), 1 382(m), 1 063(w), 670(m).

1.3 X-ray crystallography

Diffraction intensities for complexes **1** and **2** were collected on a Bruker SMART 1000 CCD diffractometer with graphite-monochromated Mo *K*α radiation (λ=0.071 073 nm) by using the ω-φ scan technique. Lorentz polarization and absorption corrections were applied. The structures were solved by direct methods and refined with the full-matrix least-squares technique using the SHELXTL-2013 program[14-15]. Anisotropic thermal parameters were assigned to all non-hydrogen atoms. The hydrogen atoms were generated geometrically. The crystallographic data and details of refinements for complexes **1** and **2** are summarized in Table 1. Selected bond lengths and angles are listed in Table 2. Corresponding hydrogen bonds lengths and angles for **1** and **2** are listed in Table 3.

CCDC: 1865772, **1**; 1486544, **2**.

Table 1　Crystal data and structure refinement information for complexes 1 and 2

	1	2
Empirical formula	$C_{20}H_{16}N_{14}Zn$	$C_{20}H_{16}N_{14}Zn$
Formula weight	517.84	517.84
Crystal system	Orthorhombic	Monoclinic

Continued Table 1

Space group	*Pbcn*	$P2_1/c$
Temperature / K	293(2)	296(2)
a / nm	1.656 48(17)	1.280 22(11)
b / nm	0.951 97(15)	0.881 69(8)
c / nm	1.383 58(16)	2.246 89(15)
β / (°)		123.209(4)
V / nm^3	2.181 8(5)	2.122 0(3)
Z	4	4
F(000)	1 056.0	1 056
D_c / ($Mg\cdot m^{-3}$)	1.576	1.621
Absorption coefficient / mm^{-1}	1.169	1.202
Data, restraint, parameter	1 925, 0, 159	4 389, 0, 316
GOF	1.007	1.031
R_1[a] [$I\geqslant 2\sigma(I)$]	0.047 1	0.031 5
wR_2[b] (all data)	0.093 0	0.080 6

[a] $R_1=\sum||F_o|-|F_c||/|F_o|$; [b] $wR_2=[\sum w(F_o^2-F_c^2)^2/\sum w(F_o^2)^2]^{1/2}$.

Table 2 Selected bond lengths (nm) and angles (°) of 1 and 2

		1			
Zn(1)-N(1)	0.198 37(17)	Zn(1)-N(5)^{i}	0.198 42(17)	Zn(1)-N(9)	0.199 77(18)
Zn(1)-N(12)^{i}	0.201 03(17)				
N(1)-Zn(1)-N(5)^{i}	108.57(7)	N(1)-Zn(1)-N(9)	100.46(7)	N(5)^{i}-Zn(1)-N(9)	113.48(8)
N(1)-Zn(1)-N(12)^{i}	127.80(8)	N(5)^{i}-Zn(1)-N(12)^{i}	102.96(7)	N(9)-Zn(1)-N(12)^{i}	103.73(7)
		2			
Zn(1)-N(2)	0.197 3(3)	Zn(1)-N(2)^{i}	0.197 3(3)	Zn(1)-N(7)^{ii}	0.199 2(3)
Zn(1)-N(7)^{iii}	0.199 2(3)				
N(2)^{i}-Zn(1)-N(7)^{ii}	108.70(13)	N(7)^{ii}-Zn(1)-N(7)^{iii}	113.0(2)	N(2)-Zn(1)-N(2)^{i}	109.6(2)
N(2)^{i}-Zn(1)-N(7)^{iii}	108.70(13)				

Symmetry codes: [i] $x+1, -y+1/2, z+1/2$ for **1**; [i] $1-x, y, 1/2-z$; [ii] $1/2+x, 1/2-y, 1-z$; [iii] $1/2-x, 1/2-y, -1/2+z$ for **2**.

Table 3 Hydrogen bond parameters for 1 and 2

D–H···A	*d*(D-H) / nm	*d*(H···A) / nm	*d*(D···A) / nm	∠DHA / (°)
		1		
C(1)–H(1)···N(6)^{i}	0.093	0.270	0.335 5(3)	128
C(2)–H(2)···N(11)^{ii}	0.093	0.235	0.324 5(3)	161
C(18)–H(18)···N(4)^{iii}	0.097	0.257	0.326 6(3)	160
C(19)–H(19)···N(10)^{iv}	0.093	0.249	0.315 5(3)	129
C(20)–H(20)···N(6)^{v}	0.093	0.241	0.312 8(3)	134
C(20)–H(20)···N(7)^{v}	0.093	0.256	0.334 5(3)	142
		2		
C(9)–H(9)···N(4)^{i}	0.093	0.230	0.319 47(5)	161

Symmetry codes: [i] $x+1, -y+1/2, z+1/2$; [ii] $-x+2, -y+1, -z+1$; [iii] $-x+1, y-1/2, -z+1/2$; [iv] $x-1, -y+1/2, z-1/2$; [v] $-x+1, -y, -z$ for **1**; [i] $-x+1/2, -y+1/2, z+1/2$ for **2**.

2 Results and discussion

2.1 Syntheses of polymorphic complexes 1 and 2

Complexes **1** and **2** are air-stable and can retain their structural integrity at room temperature for a considerable length of time. Notably, hydrothermal reaction conditions are essential for preparing **1** and **2**. HL ligand contains rich nitrogen atoms, and two nitrogen atoms of triazole moieteis and four nitrogen atoms of tetrazole moieteis can participate in coordination. As shown in Scheme 1, the L^- ligands in these coordination polymers contain the bi-dentate bridging coordination mode. For **1** and **2**, bidentate coordination modes draw the self-assembly of coordination polymers to form 1D and 2D coordination polymers. On the other hand, it is also noted that dihedral angles between triazole, phenyl and tetrazole aromatic rings are also flexible. For example, as listed in Table 4, these dihedral angles between triazole and aromatic benzene rings are 81.01(2)° in **1**, while these dihedral angles in the polymorphic complex **2** are 72.08(1)° indicating great change of these flexible dihedral angles. Flexible dihedral angles together with diverse coordination modes make the fact that we could not succeed to anticipate the self-assembly results of L^- ligand and metal ions. Therefore the building block of HL has great potential in the construction of these flexible dynamic coordination frameworks[16].

Table 4　Different flexible dihedral angles between triazole, phenyl and tetrazole aromatic rings within the multi-dentate HL ligand for 1 and 2

	Dihedral angles between triazole and aromatic benzene rings / (°)	Dihedral angles between tetrazole and aromatic benzene rings / (°)
1	81.01(2)	10.99(1)
2	72.08(1)	4.85(2)

2.2 Structure of polymorphic zinc(Ⅱ) coordination polymers $[Zn(\mu_2\text{-}L)_2]_n$ (1) and $[Zn(\mu_2\text{-}L)_2]_n$ (2)

Colorless crystals of polymorphic complexes **1** and **2** can be obtained at different hydrothermal reaction temperature (120 ℃ for **1** and 160 ℃ for **2**). **1** crystallizes in orthorhombic *Pbcn* space group while **2** crystallizes in monoclinic $P2_1/c$ space group. Complex **1** is a 1D chain zinc(Ⅱ)-L coordination framework. As shown in Fig.1 and Fig.2, each symmetric unit of the 1D framework $[Zn(\mu_2\text{-}L)_2]_n$ (**1**) contains one Zn(Ⅱ) ion in tetrahedral geometry and two bridging L^- ligand. The central Zn(Ⅱ) ion is four-coordinated by four nitrogen atoms (N(1), N(5)^i, N(9) and N(12)^i) from four L^- forming ZnN_4 donor set. The Zn-N distances are 0.198 37(17)~0.201 03(17) nm, and all the N-Zn-N angles are in a range of 100.46(7)°~127.80(8)°. Such coordination geometry is in accordance with a tetrahedral coordinated Zn(Ⅱ) center[17]. Zn(Ⅱ)⋯Zn(Ⅱ) distances across the bridging L^- ligand in **1** are 1.213(4) nm. These bridging L^- ligands connect the adjacent Zn(Ⅱ) ions forming 1D left- and right-handed helical chains. The helical pitch for these 1D helical chains is 2.302 7(8) nm. It is noted that the C–H⋯N non-classical hydrogen bonding interactions (C(1)⋯N(6)^i 0.335 5(3) nm, C(2)⋯N(11)^{ii} 0.324 48(3) nm, C(18)⋯N(4)^{iii} 0.326 6(3) nm, C(19)⋯N(10)^{iv} 0.315 5(3) nm, C(20)⋯N(6)^v 0.312 72(3) nm, C(20)⋯N(7)^v 0.334 39(3) nm) also can be found in **1** (Symmetry codes: $^i x+1, -y$

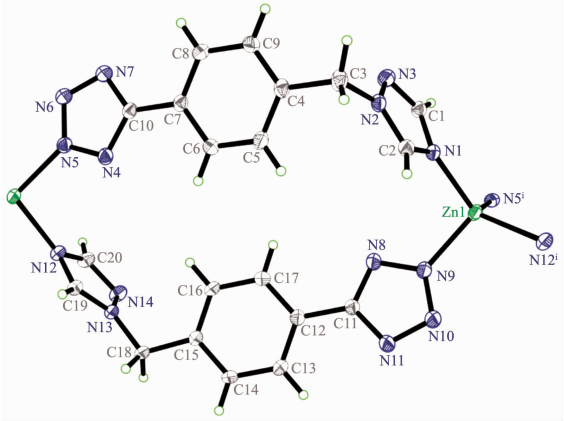

Thermal ellipsoids drawn at 30% probability level; Symmetry codes: $^i x+1, -y+1/2, z+1/2$

Fig.1　Structure of $[Zn(\mu_2\text{–}L)_2]_n$ (**1**)

+1/2, z+1/2; [ii] −x+2, −y+1, −z+1; [iii] −x+1, y−1/2, −z+1/2; [iv] x−1, −y+1/2, z−1/2; [v] −x+1, −y, −z), which also further stabilized the 1D coordination chain of **1**.

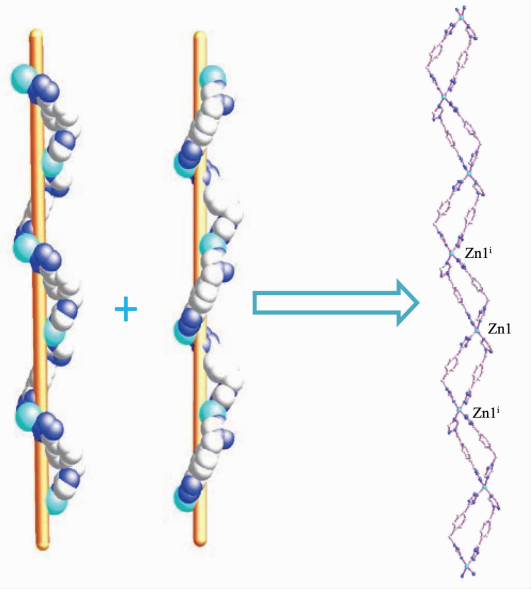

Symmetry codes: [i] x−1, −y+1/2, z−1/2

Fig.2 Left- and right-handed single helical chains in $[Zn(\mu_2\text{-}L)_2]_n$ (**1**)

Complex **2** is a polymorphic 2D zinc (Ⅱ)-L framework, in which central Zn(Ⅱ) ions are also linked by the bridging L^- ligands (Fig.3). As shown in Fig.3 and 4, The fundamental structural unit of **2** contains one Zn(Ⅱ) ion in tetrahedral geometry and two bridging L^- ligands. The central Zn(Ⅱ) ion is four-coordinated by four nitrogen atoms (N(2), N(2)[i], N(7)[i] and N(7)[ii]) from four L^- forming ZnN_4 donor set. The Zn-N distances are 0.197 3(3)~0.199 2(3) nm, and all the N-Zn-N angles are in a range of 108.43(13)°~113.0(2)°. Such coordination geometry is in accord with a tetrahedral coordinated Zn(Ⅱ) centers. The Zn(Ⅱ)⋯Zn(Ⅱ) distance across the bridging L^- ligand in **2** is

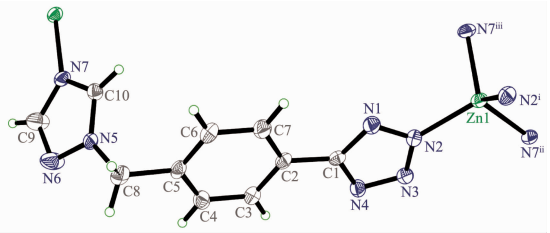

Thermal ellipsoids drawn at 30% probability level; Symmetry codes: [i] 1−x, y, 1/2−z; [ii] 1/2+x, 1/2−y, 1−z; [iii] 1/2−x, 1/2−y, −1/2+z

Fig.3 Fundamental structural unit of $[Zn(\mu_2\text{-}L)_2]_n$ (**2**)

1.173 0(1) nm. All the N-Zn-N and N-Zn-O angles are in the normal range, such coordination geometry is in accord with a four-coordinated Zn(Ⅱ) centers.

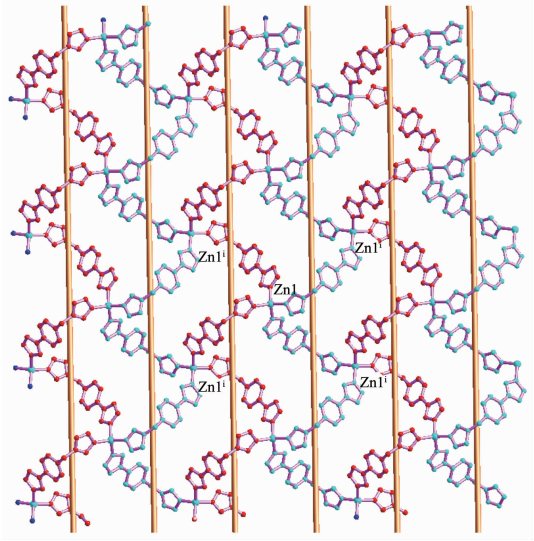

Symmetry codes: [i] 1/2−x, 1/2−y, 1/2+z

Fig.4 Two dimensional coordination framework of $[Zn(\mu_2\text{-}L)_2]_n$ (**2**) containing alternative 1D right-handed and left-handed helical chains

As shown in Fig.4, the 1D left- and right-handed helical chains can also be observed, which are further interlinked via central zinc (Ⅱ) ions forming a two-dimensional (2D) coordination framework. The helical pitches for these 1D helical chains are 1.382 6(2) nm. It is noted that the C−H⋯N non-classical hydrogen bonding interactions (C(9)⋯N(4)[i], 0.319 47(5) nm) also can be found in **2** (Symmetry codes: [i] −x+1/2, −y+1/2, z+1/2), which also further stabilized the 2D coordination framework of **2**.

2.3 Photoluminescent emission spectroscopy of 1 and 2

Inorganic-organic hybrid coordination polymers have been investigated for fluorescence properties and for potential applications as luminescent materials, such as light-emitting diodes (LEDs)[18]. Owing to the ability of affecting the emission wavelength and strength of organic materials, syntheses of inorganic-organic coordination polymers by the judicious choice of conjugated organic spacers and transition metal centers can be an efficient method for obtaining new types of electroluminescent materials, especially for

d^{10} or d^{10}-d^{10} systems. In the present work, we have explored the luminescent properties of HL and organic/inorganic coordination polymers **1** and **2** based on the ligands in aqueous solutions.

As shown in Fig.5, at ambient temperature, the free ligands HL in the aqueous solutions were luminescent and showed the broad emission maximum at 303 nm (λ_{max}=260 nm). The chromospheres are the aromatic rings and the observed emission is ascribed to π-π* transition. The fluorescence spectra of **1** and **2** at room temperature have been determined. In comparison with that of free HL, the main emission bands of complexes **1** and **2** also almost were located at the same position exhibiting fluorescence (λ_{max}=260 nm) with slightly different band shape, which also should be ascribed to intra-ligand fluorescent emissions. The syntheses of new polymorphic Zn(Ⅱ) complexes with the combination of triazole and tetrzole bi-functional groups can be an efficient method for obtaining new types of luminescent materials. On the other hand, in order to examine the stability of **2** in aqueous solutions, the resulting materials were dispersed in water followed by the fluorescence intensity measurement at different time intervals. The fluorescence intensity ratio was independent of time and almost remained constant within 12 h indicating **2** can behave good fluorescent stability. The good fluorescent stability results from good solvent stability and dispersibility of complex **2** in aqueous solution. Therefore, **2** can be employed as a prominent candidate for fluorescent detection in aqueous solution.

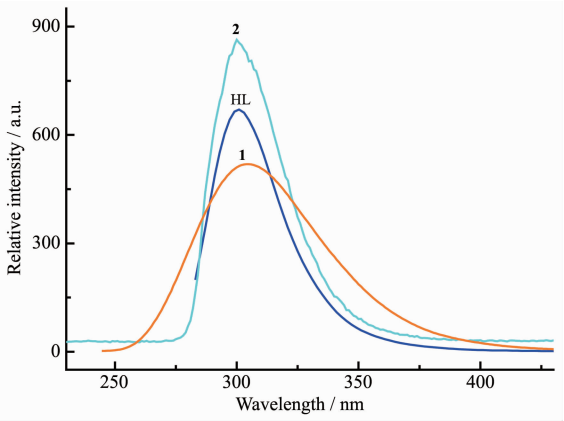

Fig.5　Photoluminescent spectra of HL and complexes **1** and **2**

2.4　Photoluminescent sensing PA by complex 2

To explore the potential of **2** toward the sensing of PA, its luminescence properties were further investigated. The solvent suspension of **2** were prepared by placing its finely ground samples (3 mg) into 4 mL of H_2O, then PA was further added into the resulting aqueous solutions. As shown in Fig.6a, it is noted that the emission intensities of solvent suspensions were largely dependent on the addition of PA, which exhibits a significant quenching effect, resulting in nearly photoluminescence quenching. These results indicated that complex **2** can be used as a luminescent probe for detecting PA molecules. Moreover, powder XRD analysis of **2** after immersing it in different analytes revealed that the original framework structure is retained.

To further investigate the quenching effect of PA molecules on the luminescence intensity of **2**, complex **2** was dispersed in aqueous solutions as the standard emulsion, then the analyst PA gradually increased while the emissive response was monitored. It is obvious that the photoluminescent intensity of **2** gradually decreases with the addition of PA (Fig.6b and 6c)[19]. For **2**, with the addition of 1 mmol·L^{-1} PA to the aqueous emulsion, the corresponding emission intensity is attenuated by approximately 42.15%, and the emission spectra shows 74.3% photoluminescent quenching after the addition of 1.4 mmol·L^{-1} PA.

In order to further display the detection sensitivity, the photoluminescent quenching efficiency can be rationalized using Stern-Volmer (SV) equation: $I_0/I=K_{SV}c_A+1$, where I_0 and I are the suspension luminescence intensities of complex **2** without and with the addition of the analyte, respectively, c_A is the concentration of analyte, and K_{SV} is the quenching coefficient. The Stern-Volmer plot for PA is typically linear at low concentrations, and the K_{SV} value for PA can be calculated (For **2**: 3.65×10^3 L·mol^{-1}). The high sensitivity of the photoluminescent response of **2** to PA shows that these Zn(Ⅱ) coordination frameworks could be used as the excellent sensors for identifying and quantifying these PA molecules. As we all know, the practical applications of sensors are always restricted, since luminescent probes are costly and can be hard

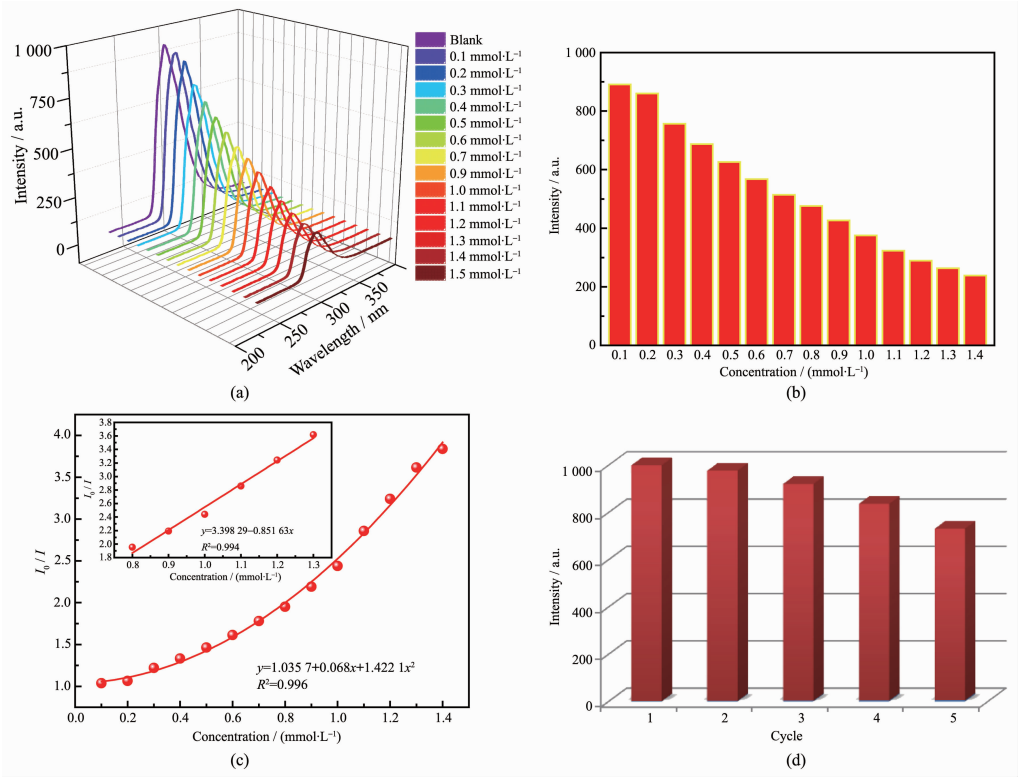

Fig.6 (a) Photoluminescent spectra of **2** in the absence and presence of PA with different concentrations; (b) Photoluminescent intensity of **2** at 303 nm in the presence of PA with different concentrations; (c) Linear correlation of luminescence intensity vs PA concentration; (d) Recyclable photoluminescent detection of PA by **2**

to reuse. Hence, fast and simple regeneration methods are important for luminescent probe applications. Herein, to investigate the recyclable performance of **2**, we attempted to immerse **2** in an aqueous solution of 1 mmol·L^{-1} PA for 20 s to completely form **2**-PA, and then **2**-PA was washed with water several times. Five runs were performed (Fig.6d), while the luminescence intensity and the PXRD pattern of the recycled **2** were well consistent with the original **2** (Supporting Information, Fig.S1). The results clearly showed that **2** can be recycled by a fast and simple method, and the framework of **2** still remains intact, indicating that **2** is a recyclable probe for detecting PA[20-21].

Although various analytical and spectroscopic methods have been developed for the detection of PA, a simple and rapid technique using Zn(Ⅱ) coordination framework **2** might be an ideal photoluminescent sensing platform, since it seems more attractive by virtue of its high sensitivity, simple operation, rapid response time and cost effectiveness.

3 Conclusions

In conclusion, a flexible bi-functional multi-dentate 5-(4-((1*H*-1,2,4-triazol-1-yl)methyl)phenyl)-1*H*-tetrazole (HL) has been employed, to obtain two novel polymorphic one- and two-dimensional zinc(Ⅱ) coordination polymers, namely $[Zn(\mu_2\text{-}L)_2]_n$ (**1**) and $[Zn(\mu_2\text{-}L)_2]_n$ (**2**). **1** and **2** present temperature induced polymorphic zinc(Ⅱ)-L 1D (**1**) and 2D (**2**) coordination frameworks. Furthermore, the luminescence properties of **1** and **2** have been investigated, indicating strong photoluminescent emissions. Additionally, photoluminescent measurements illustrate that complex **2** exhibits highly sensitive luminescence for PA in aqueous solution with high quenching efficiency (K_{SV}=3.65×10^3 L·mol^{-1}) and low detection limit (3.004 μmol·L^{-1}, *S*/*N*=3). The results also reveal great potential in the construction of these flexible frameworks employing these semi-rigid multi-dentate ligands as basic building blocks. On the basis of this work, the syntheses, structures and properties studies of these coordination

polymers using HL as basic building blocks are also under way in our laboratory.

Supporting information is available at http://www.wjhxxb.cn

References:

[1] (a)Banerjee R, Phan A, Wang B, et al. *Science*, **2008**,**319**:939-943
(b)Zhu P P, Sun L J, Sheng N, et al. *Cryst. Growth Des.*, **2016**,**16**:3215-3223
(c)Bijelic A, Rompel A. *Acc. Chem. Res.*, **2017**,**50**:1441-1448

[2] (a)Anjass M H, Kastner K, Nagele F, et al. *Angew. Chem. Int. Ed.*, **2017**,**56**:14749-14752
(b)He W W, Li S L, Zang H Y, et al. *Coord. Chem. Rev.*, **2014**,**279**:141-160
(c)Wang X, Zhang Q, Nam C, et al. *Angew. Chem. Int. Ed.*, **2017**,**56**:11826-11829

[3] (a)Yi X F, Izarova N V, Stuckart M, et al. *J. Am. Chem. Soc.*, **2017**,*139*:14501-14510
(b)Bunzen H, Kolbe F, Kalytta-Mewes A, et al. *J. Am. Chem. Soc.*, **2018**,**140**:10191-10197

[4] (a)Zhang Z M, Duan X P, Yao S, et al. *Chem. Sci.*, **2016**,**7**:4220-4229
(b)Moran C M, Joshi J N, Marti R M, et al. *J. Am. Chem. Soc.*, **2018**,**140**:9148-9153
(c)Yu Y, Zhang Q, Buscaglia J M. *Analyst*, **2016**,**141**:4424-4431
(d)Zhang Q, Kaisti M, Prabhu A, et al. *Electrochim. Acta*, **2017**,**261**:256-264

[5] (a)Kaisti M, Zhang Q, Levon K, et al. *Sens. Actuators B*, **2017**, **241**:321-326
(b)Yu Y, Zhang Q, Wang Y, et al. *Analyst*, **2016**,**141**:5607-5617
(c)Fu H, Qin C, Lu Y, et al. *Angew. Chem. Int. Ed.*, **2012**, **51**:7985-7989
(d)Genovese M, Lian K. *J. Mater. Chem. A*, **2017**,**5**:3939-3947
(e)Gui S L, Huang Y Y, Hu F, et al. *Anal. Chem.*, **2018**,**90**:9708-9715

[6] Du P Y, Lustig W P, Teat S J, et al. *Chem. Commun.*, **2018**, **54**:8088-8091

[7] Hu P, Yin L, Kirchon A, et al. *Inorg. Chem.*, **2018**,**57**:7006-7014

[8] (a)Naskar B, Bauza A, Frontera A, et al. *Dalton Trans.*, **2018**, **47**:15907-15916
(b)Xu C, Huang H P, Ma J X, et al. *New J. Chem.*, **2018**,**42**:15306-15310
(c)Yang Y, Song X R, Xu C, et al. *Dalton Trans.*, **2018**,**47**:11077-11083
(d)Wang J, Zhang L W, Bao L, et al. *Dyes Pigm.*, **2018**,**150**:301-350
(e)Arici M. *Cryst. Growth Des.*, **2017**,**17**:5499-5505
(f)HuY L, Ding M L, Liu X Q, et al. *Chem. Commun.*, **2016**, **52**:5734-5737
(g)Mostakim S K, Biswas S. *CrystEngComm*, **2016**,**18**:3104-3113

[9] Das P, Mandal S K. *J. Mater. Chem. A*, **2018**,**6**:16246-16256

[10](a)Ding B, Liu S X, Cheng Y, et al. *Inorg. Chem.*, **2016**,**55**:4391-4402
(b)Wang X R, Du J, Huang Z. *J. Mater. Chem. B*, **2018**,**6**:4569-4574
(c)Wang X R, Huang Z, Du J, et al. *Inorg. Chem.*, **2018**,**57**:12885-12899
(d)Ding B, Zhang H M, Li X S, et al. *Dyes Pigm.*, **2018**,**159**:187-197
(e)Cheng Y, Wu J, Guo C, et al. *J. Mater. Chem. B*, **2017**,**5**:2524-2535
(f)Ding B, Cheng Y, Wu J, et al. *Dyes Pigm.*, **2017**,**146**:455-466

[11]Haasnoot J G. *Coord. Chem. Rev.*, **2000**,**200-202**:131-185

[12]Li X X, Xu H Y, Kong F Z, et al. *Angew. Chem. Int. Ed.*, **2013**,**52**:13769-13773

[13](a)Gusev A N, Nemec I, Herchel R, et al. *Dalton Trans.*, **2014**,**43**:7153-7163
(b)Naik A D, Marchand-Brynaert J, Garcia Y. *Synthesis*, **2008**,**1**:149-154
(c)Mattews B R, Edward S R, Johnston B L. *US Patent*, *BG*45700*A*3. 1989-07-14.

[14]Sheldrick G M. *Acta Crystallogr. Sect. A*: *Found. Crystallogr.*, **2008**,**A64**:112-122

[15]Dolomanov O V, Bourhis L J, Gildea R J, et al. J. *Appl. Crystallogr.*, **2009**,**42**:339-341

[16](a)Santos-Figueroa L E, Moragues M E, Climent E, et al. *Chem. Soc. Rev.*, **2013**,**42**:3489-3613
(b)Miao P, Wang B, Yu Z, et al. *Biosens. Bioelectron.*, **2015**, **63**:365-370

[17](a)Ding B, Yi L, Cheng P, et al. *Inorg. Chem.*, **2006**,**45**:5799-5803
(b)Liu J Y, Wang Q, Zhang L J, et al. *Inorg. Chem.*, **2014**,**53**:5972-5985

[18]Senchyk G A, Lysenko A B, Domasevitch K V, et al. *Inorg. Chem.*, **2017**,**56**:12952-12966

[19]Liu W, Huang X, Xu C, et al. *Chem. Eur. J.*, **2016**,**22**:18769-18776

[20]Xu X Y, Yan B. *Adv. Funct. Mater.*, **2017**,**27**:1700247

[21]Wang H, Lustig W P, Li J. *Chem. Soc. Rev.*, **2018**,**47**:4729-4756